

Molecular Sieve Synthesis using Imidazolium Structure Directing Agents

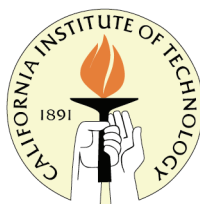
Thesis by

Raymond Humphrey Archer

In Partial Fulfillment of the Requirements for the

degree of

Doctor of Philosophy



California Institute of Technology

Pasadena, California

2009

(Defended May 29, 2009)

© 2009

Raymond Humphrey Archer

All Rights Reserved

Acknowledgements

I would like to thank my advisor, Professor Mark Davis, for his contribution throughout my graduate career. Through the many disappointments and failed projects he always had suggestions and ideas on how to move forward. I would also like to thank the other members of my committee, Professor Dave Tirrell, Dr. Jay Labinger, and Dr. Stacey Zones. I am particularly indebted to Stacey for his time and contribution to all aspects of this thesis. I am particularly glad I made the effort to visit with him when I was in the Bay Area over the last 11 months. Our various meetings in Richmond, Berkeley, and the Beach Chalet were valuable to my research and offered a different perspective on what life might entail after graduate school. I am also indebted to the help Allen Burton provided, particularly with the molecular modeling and for his keen eye to look at X-ray patterns. All work presented in this thesis received financial support from the Chevron Energy Research Company and the constant support is appreciated.

I would also like to thank the members of the Davis Group, both past and present, for their help and guidance. Most of the training I received was from Hyunjoo Lee and Jon Galownia and they both made Room 31 a pleasant office. John Carpenter also deserves credit for running the CI tests on my materials. Another person I would like to thank is Sonjong Hwang for his help with solid-state NMR experiments. Tom Dunn and Larry Henling were always willing to help troubleshoot equipment and their assistance helped to speed repairs. Through the many projects I was involved with I received valuable assistance from Mona Shahgholi, Nathan Dalleska, Bill Tivol, and Carol Garland.

Finally, I could not have completed my studies without the love and support of my family. My parents and siblings have been a source of constant support from my formative school years through the University of Canterbury and on to Caltech. My time at Caltech would have been far less enjoyable without my wife, Melissa, to share the experience and I cannot wait to be reunited with her in the near future. Also, the welcome her family gave me was appreciated, being so far from home.

Abstract

The synthesis of high-silica molecular sieve SSZ-70 is investigated through a guest/host study of imidazolium structure directing agents (SDAs). The original borosilicate synthesis is extended to pure-silica and aluminosilicate compositions using six imidazolium SDAs. Physical characterization using powder X-ray diffraction (XRD), ^{29}Si solid-state NMR, electron microscopy, thermogravimetric analysis, and nitrogen adsorption shows SSZ-70 to be layered with similarity to MCM-22 (MWW). Aluminum-containing SSZ-70 is evaluated for catalytic activity using the constraint index (CI) test and shows a similar cracking rate to SSZ-25 (MWW structure). Distinct differences in CI as a function of time on stream are observed between MWW and SSZ-70 materials. Additional molecular sieve phases observed in this guest/host study included Theta-1 (TON), ZSM-5 (MFI), ZSM-23 (MTT), ZSM-12 (MTW), Beta, Mordenite (MOR), CIT-5 (CFI), SSZ-16 (AFX), and SSZ-35 (STF).

Attempts to synthesize Beta enriched in chiral polymorph A are investigated in a second guest/host study using five chiral imidazolium SDAs. Two SDAs successfully gave Beta, but no enrichment in polymorph A is observed. The remaining SDAs do not direct the formation of any molecular sieve phases. Molecular modeling indicates both SDAs occupy the straight [100]/[010] 12 membered ring (MR) pores of Beta. In this configuration, no chirality could be projected across the [001] fault planes and this offers an explanation for not observing enrichment. Modeling shows careful consideration must be given to efficiently filling the entire void volume when large SDAs are used. Additional molecular sieve phases observed in the guest/host study are EU-1 (EUO) and MOR.

Finally, attempts to synthesize novel materials using supramolecular SDAs are described. Supramolecular SDAs are created through adamantyl/ β -cyclodextrin inclusion complex formation. Both 2:1 and 1:1 inclusion complex stoichiometries are attempted. Significant cyclodextrin degradation occurs at temperatures above 90°C and no structure-directing effect can be attributed to the cyclodextrin. Molecular sieve phases observed in the study are SSZ-16 (AFX), MOR, B-SSZ-13 (CHA), VPI-8 (VET), and SSZ-24 (AFI).

Table of Contents

Acknowledgements	iii
Abstract	v
Table of Contents.....	vii
List of Figures	ix
List of Tables	xiv
Chapter One: Introduction.....	1
1.1: Molecular Sieve Synthesis.....	1
1.2: Previous Examples of Imidazolium Structure Directing Agents.....	6
1.2: Thesis Overview.....	9
1.3: References	10
Chapter Two: Imidazolium Structure Directing Agents in Molecular Sieve Synthesis: Exploring Guest/Host Relationships in the Synthesis of SSZ-70	13
2.1: Introduction	13
2.2: Experimental Section	19
2.2.1: Structure Directing Agent Synthesis	19
2.2.2: Inorganic Reactions	26
2.2.3: Product Characterization.....	28
2.2.4: Catalytic Testing	29
2.3: Results and Discussion.....	30
2.3.1: Results Overview	30
2.3.2: SSZ-70 Characterization.....	45
2.3.3: Catalytic Activity	66

2.4: Conclusions	69
2.5: Acknowledgments	70
2.6: References	70
Chapter Three: Guest/Host Relationships using Chiral Imidazolium Structure Directing Agents in Molecular Sieve Synthesis.....	
3.1: Introduction	75
3.2: Experimental Section	83
3.2.1: Structure Directing Agent Synthesis	83
3.2.2: Inorganic Reactions	86
3.2.3: Molecular Modeling	87
3.2.4: Product Characterization.....	88
3.3: Results and Discussion.....	88
3.4: Conclusions	111
3.5: References	112
Chapter Four: Supramolecular Structure Directing Agents <i>via</i> Adamantyl/Cyclodextrin Inclusion Complexes	
4.1: Introduction	117
4.2: Experimental.....	123
4.3: Results and Discussion.....	125
4.4: Conclusions	142
4.5: References	143
Chapter Five: Conclusions and Future Considerations	
5.1: References	150

List of Figures

Figure 1.1: Schematic of Brønsted acid site	2
Figure 1.2: Scheme for Si-MFI-TPA crystallization (from Reference 13).....	4
Figure 2.1: Imidazolium Structure Directing Agents Studied.....	17
Figure 2.2: ^{13}C CP-MAS NMR of products obtained using 1,3-bis(1-adamantyl) imidazolium SDA 15 . Top to bottom=CIT-5, SSZ-35, SSZ-16 and SDA $^+\text{Cl}^-$. The inset enlarges the imidazolium region	41
Figure 2.3: Phases obtained in NaY reactions as a function of NaOH/SiO $_2$ ratio for bis(cyclohexyl) SDA 8 (■), bis(<i>t</i> -butyl) SDA 4 (●), bis(isooctyl) SDA 12 (▲) and bis(adamantyl) SDA 15 (▼). AMO indicates amorphous and residual NaY is not shown.....	43
Figure 2.4: XRD patterns for germanosilicate reactions using 4 , 8 , 12 and 15 . Top to bottom= 4 (Beta+ISV), 8 (Beta), 12 (amorphous) and 15 (amorphous).....	45
Figure 2.5: XRD patterns for top to bottom; SSZ-25, Al-SSZ-70 (F) and Al-SSZ-70 (OH)	47
Figure 2.6: XRD patterns from 2–12°2 θ for top to bottom; SSZ-25, Al-SSZ-70 (F) and Al-SSZ-70 (OH)	48
Figure 2.7: XRD patterns of calcined SSZ-70 products. Top to bottom; Si-SSZ-70(F), Al-SSZ-70 (F) and B-SSZ-70 (F)	49
Figure 2.8: Solid-state ^{29}Si NMR spectra of Si-SSZ-70. Top to bottom: Si-SSZ-70(OH) CP-MAS, Si-SSZ-70(OH) BD-MAS, Si-SSZ-70(F) CP-MAS and Si-SSZ-70(F) BD-MAS.....	51
Figure 2.9: Solid-state ^{29}Si BD-MAS NMR of calcined Si-SSZ-70(F).....	52

Figure 2.10: SEM images of as-made Si-SSZ-70 (left) and calcined Si-SSZ-70 (right)	55
Figure 2.11: TEM image of B-SSZ-70	56
Figure 2.12: TGA of Si-SSZ-70(F) synthesized using 5 (red) and 8 (black) ..	62
Figure 2.13: TGA of post-synthesis treatments for Al-SSZ-70(OH) synthesized using 8 . Black=parent material, blue=DMF extracted and red=350°C treated.	63
Figure 2.14: XRD patterns of post-synthesis treatments for Al-SSZ-70(OH) synthesized using 8 . Bottom to top: parent material, DMF extracted and 350°C treated	64
Figure 2.15: CI test cracking rate vs. time on stream for Al-SSZ-70 materials. SSZ-25(▼), Al-SSZ-70(F)(●), Al-SSZ-70(OH-5)(▲), Al-SSZ-70(OH-8)(■) and Al-SSZ-70(OH-8 350°C treated)(◀)	68
Figure 2.16: Constraint index vs. time on stream for Al-SSZ-70 materials. SSZ-25(▼), Al-SSZ-70(F)(●), Al-SSZ-70(OH-5)(▲), Al-SSZ-70(OH-8)(■) and Al-SSZ-70(OH-8 350°C treated)(◀)	69
Figure 3.1: Beta building layer and representations of Polymorphs A, B and C. For clarity oxygen atoms have been omitted. Solid lines connect neighboring silicon atoms in each layer unit and dashed lines connect silicon atoms in adjacent layers	76
Figure 3.2: Simulated XRD patterns for Beta polymorphs A and B. Bottom to top=100% polymorph B (p(A)=0) to 100% polymorph A (p(A)=1))	78
Figure 3.3: Chiral imidazolium SDAs studied	80
Figure 3.4: XRD patterns of pure silica Beta products using 17 and 19 at H ₂ O/SiO ₂ =3.5. Top=regular Beta obtained with 19 and bottom=odd Beta pattern using 17 with distinct asymmetry in the low angle reflection	91

Figure 3.5: Borosilicate hydroxide XRD patterns. Top=Beta with asymmetry in the low angle reflection using 19 and bottom shows EU-1 plus minor layered using 17	92
Figure 3.6: ^{13}C CP-MAS NMR of Beta products using 19 . Top to bottom: Pure silica fluoride at $\text{H}_2\text{O}/\text{SiO}_2=3.5$, aluminosilicate hydroxide (SAR=50), borosilicate hydroxide (seeded) and liquid ^{13}C NMR of tetrafluoroborate salt (asterisk denotes NMR solvent resonances)	99
Figure 3.7: ^{13}C CP-MAS NMR of Beta products using 17 . Top spectra shows liquid ^{13}C NMR of chloride salt (asterisk denotes NMR solvent resonances) and bottom shows ^{13}C CP-MAS NMR of Beta product	100
Figure 3.8: Liquid ^{13}C NMR of SDA 18 and ^{13}C CP-MAS NMR of products using 18 . Top to bottom=liquid NMR spectrum, B-Beta reaction product and pure-silica product at $\text{H}_2\text{O}/\text{SiO}_2=3.5$. * denotes resonances from the NMR solvent and + indicates spinning side-band	105
Figure 3.9: Energy-minimized location of 17 in EUO. Left panel shows [001] view perpendicular to [100] 10MR pore, right panel shows [100] view along 10MR pore	108
Figure 3.10: Energy-minimized location of 17 in *BEA	109
Figure 3.11: Energy minimized location of 19 in *BEA	110
Scheme 4.1: β -cyclodextrin structure and three-dimensional pictorial description	119
Scheme 4.2: Proposed 2:1 inclusion complex between β -CD and 1,3-bis(1-adamantyl)imidazolium 15	120
Scheme 4.3: MCM-41 formation schematic	121

Scheme 4.4: Supramolecular SDA used to synthesize pure-silica LTA (ITQ-29)	122
Scheme 4.5: Sodium/18-crown-6 complex.....	123
Figure 4.1: Isothermal titration calorimetry plot of 1,3-bis(1-adamantyl)imidazolium chloride/ β -cyclodextrin guest/host complex	126
Figure 4.2: Plot of pH versus reaction time for SAR=35 reactions with no cyclodextrin and Me-O- β -CD. NaOH/SiO ₂ =0.25+CD/SiO ₂ =0.0 (■), NaOH/SiO ₂ =0.25+CD/SiO ₂ =0.4 (●), NaOH/SiO ₂ =0.05+CD/SiO ₂ =0.0 (▲) and NaOH/SiO ₂ =0.05+CD/SiO ₂ =0.4 (▼)	128
Figure 4.3: XRD patterns for 1,3-bis(1-adamantyl)imidazolium hydroxide/ β -cyclodextrin inclusion complex. Top= Me-O- β -CD (SSZ-16), middle = β -CD (amorphous) and bottom = no cyclodextrin (SSZ-16 + minor NaY).....	129
Figure 4.4: XRD patterns for borosilicate reactions employing N,N,N-trimethyl-1-adamantanammonium hydroxide/Me-O- β -CD inclusion complex as SDA. Top=Adamantyl SDA/Me-O- β -CD complex (amorphous + CHA) and bottom=Adamantyl SDA only (CHA)	133
Figure 4.5: XRD patterns for zincosilicate reactions employing N,N,N-trimethyl-1-adamantanammonium hydroxide/Me-O- β -CD inclusion complex as SDA. Top=Adamantyl SDA/Me-O- β -CD complex + GeO ₂ (VET+layered) and bottom=Adamantyl SDA/Me-O- β -CD complex (VET).....	136
Figure 4.6: XRD patterns of unknown dense aluminophosphate phase. Top to bottom=Adamantyl SDA/ β -CD complex, adamantyl SDA/Me-O- β -CD and adamantyl SDA only	142

Scheme 5.1: Proposed synthesis of ^{13}C -labeled imidazolium SDA..... 148

List of Tables

Table 2.1: Phases obtained from pure silica fluoride reactions at 150°C	32
Table 2.2: Phases obtained from borosilicate fluoride reactions at 150°C	34
Table 2.3: Phases obtained from borosilicate hydroxide reactions at 150°C ..	36
Table 2.4: Phases obtained from aluminosilicate hydroxide syntheses at 150°C	38
Table 2.5: Phases obtained from pure silica fluoride syntheses at 175°C	39
Table 2.6: Phases obtained from hydroxide syntheses at 170°C.....	39
Table 2.7: ²⁹ Si chemical shifts and relative intensities for as-made Si-SSZ-70(OH), Si-SSZ-70(F) and ITQ-1.....	53
Table 2.8: ²⁹ Si chemical shifts and relative intensities for calcined Si-SSZ-70(F) and ITQ-1	53
Table 2.9: Phase summary for chemical analysis of pure-silica fluoride products using 5 , 6 and 11	57
Table 2.10: Carbon and nitrogen content for pure-silica fluoride products using 5 , 6 and 11	58
Table 2.11: Fluoride content for pure-silica fluoride products using 5 , 6 and 11	58
Table 2.12: Chemical analysis of B-SSZ-70(F), Al-SSZ-70(F) and Al-SSZ-70(OH) products synthesized using 5	60
Table 2.13: Textural properties of SSZ-70 products	65
Table 3.1: Examples of chiral SDAs used in molecular sieve synthesis and SDAs used to synthesize enriched Beta products	81
Table 3.2: Phases obtained in pure silica fluoride reactions using chiral imidazolium SDAs	90

Table 3.3: Phases obtained in aluminosilicate and borosilicate hydroxide reactions using chiral imidazolium SDAs	92
Table 3.4: Summary of additional inorganic reaction attempts using 19	96
Table 3.5: Thermogravimetric analysis of inorganic reaction products using 17 and 19	98
Table 3.6: Summary of additional inorganic reaction attempts using 18	102
Table 3.7: Carbon, Nitrogen and Fluorine content of amorphous products from pure silica fluoride reactions 18	104
Table 3.8: Phases obtained from silicoaluminophosphate (SAPO) inorganic reactions using 17 and 19	106
Table 4.1: β -cyclodextrin/1,3-bis(1-adamantyl)imidazolium binding stoichiometry, equilibrium constant and enthalpy	125
Table 4.2: Products obtained from inorganic reactions using 1,3-bis(1-adamantyl)imidazolium hydroxide / β -cyclodextrin inclusion complexes. Gel compositions were 1.0 SiO ₂ :0.029 Al ₂ O ₃ :0.20 SDA ⁺ OH ⁻ :x CD:y NaOH:30.0 H ₂ O (x=0.0 or 0.40)	128
Table 4.3: Aluminosilicate and borosilicate reactions employing N,N,N-trimethyl-1-adamantanammonium hydroxide (SDA ⁺ OH ⁻) / β -cyclodextrin inclusion complex as structure directing agent	132
Table 4.4: Zincosilicate reactions employing N,N,N-trimethyl-1-adamantanammonium hydroxide (SDA ⁺ OH ⁻) / β -cyclodextrin inclusion complex as structure directing agent	134
Table 4.5: Gel compositions and product phases for miscellaneous reactions employing cyclodextrins	137